

## Optimisation of ECX permeation barriers towards thicker alumina

Carsten Schroer<sup>\*</sup>, Julia Lorenz, Olaf Wedemeyer, Aleksandr Skrypnik, Kateryna Khanchych

Karlsruher Institut für Technologie (KIT), Institut für Angewandte Materialien – Angewandte Werkstoffphysik (IAM-AWP), Hermann-von-Helmholtz-Platz 1, 76344 Eggenstein-Leopoldshafen, Germany

### ARTICLE INFO

#### Keywords:

Magnetic-confinement fusion  
Breeding blanket  
Tritium  
Electroplating  
Ionic liquid  
Aluminium

### ABSTRACT

The current development with respect to modifying the ECX (electrochemical X-deposition) process towards thicker alumina formed by heat treatment of aluminium electroplated on steel is described. As anticipated, changing the heat treatment atmosphere from argon to air or prolonging holding at high temperature (980 °C) increases the amount of alumina, but exposure to liquid lithium–lead eutectic reveals weak spots present in the alumina layers. The thickness of alumina produced is in the range of 1–2 μm for holding at 980 °C in air for 0.5–2 h.

### 1. Introduction

As there is no abundant natural source of the hydrogen isotope tritium ( ${}^3\text{H}$  or T), harvesting energy from thermonuclear fusion with deuterium ( ${}^2\text{H}$  or D) necessarily requires tritium production. In magnetic-confinement fusion [1], the tritium production is accomplished right in the reactor, via the interaction of neutrons released inside the reaction chamber and lithium, especially  ${}^6\text{Li}$ , provided in the associated (tritium-) breeding blanket. However, hydrogen isotopes are small and, therefore, tend to penetrate or permeate through structural materials, notably steel, which must be avoided as much as possible, not only because tritium is a generally hazardous substance to be kept enclosed inside the reactor but also in order to gather this isotope in amounts sufficient to continuously run the fusion reaction. Hence, a kind of tritium-permeation barrier (TPB) is required especially on the components of the breeding blanket, so that the best part of tritium produced arrives at the reactor unit for controlled tritium extraction. Such barrier is to be applied on the side of tritium breeding (tritium source), as plain accumulation in the structural material of the radioactive and, for the fusion process, precious isotope is already unwanted.

An appropriate TPB material typically excels in low solubility and diffusivity of hydrogen isotopes. High retention of the latter at the interface with the substrate (structural material) may compensate for some weakness in the other two properties. Because of the importance of hydrogen isotope permeation for thermonuclear fusion as well as for other processes of high technological and industrial interest, a number of materials have been characterised in respect of their potential as TPB

[2–6], pointing to certain oxides, nitrides and carbides as well as some metals, e.g., tungsten (W). Further requirements such as the tolerance of unprecedented neutron irradiation at a minimum of neutron absorption (activation of the TPB, neutronic balance of the blanket), chemical resistance against the breeding material/atmosphere or thermo-mechanical compatibility with the substrate material follow from the service situation in the breeding blanket. It should be noted that especially the irradiation load significantly decreases with increasing distance from the reaction chamber and is likely to be negligible in the tritium extraction and removal sub-system (TER) of the fusion reactor [7]. Bi- or multi-layer approaches may solve issues relating to chemical [8,9] or thermo-mechanical [10] incompatibility. Finally, an appropriate deposition process for producing a defect-free coating on the components of given geometry and size must exist.

The current TPB development in the framework of the EUROfusion programme focuses on alumina ( $\text{Al}_2\text{O}_3$ ), especially for breeding blankets in which the wanted tritium will be produced with the aid of an eutectic lithium (Li)–lead (Pb) alloy [11]. Alumina may exist in a number of crystallographic modifications, of which corundum or  $\alpha\text{-Al}_2\text{O}_3$  is the ultimately stable one [12,13]. The latter is considered having properties most favourable for service as TPB. A weak spot regarding application to the breeding blanket of  $\alpha\text{-Al}_2\text{O}_3$  is its hexagonal crystal structure, which, under the intense neutron irradiation in the blanket and especially for polycrystalline and equiaxed  $\alpha\text{-Al}_2\text{O}_3$ , gives rise to anisotropic swelling and subsequent damage [14]. Furthermore, alumina generally tends to absorb Li and form the corresponding ternary oxide, most notably for Li present in eutectic Li–Pb, against which the binary oxide is

<sup>\*</sup> Corresponding author.

E-mail address: [carsten.schroer@kit.edu](mailto:carsten.schroer@kit.edu) (C. Schroer).

<https://doi.org/10.1016/j.nme.2024.101581>

Received 2 November 2023; Received in revised form 19 December 2023; Accepted 4 January 2024

Available online 6 January 2024

2352-1791/© 2024 The Authors. Published by Elsevier Ltd. This is an open access article under the CC BY license (<http://creativecommons.org/licenses/by/4.0/>).

thermodynamically unstable under any condition relevant to breeding tritium [15]. The major concern about Li uptake is the subsequent interaction with neutrons, formation of tritium and helium as well as associated caloric effects, locally inside the TPB rather than the anticipated change in permeability or general thermo-mechanical compatibility with the substrate material. As for tolerance of neutron irradiation, which is typically higher for cubic crystal structure [14], metastable  $\gamma$ - $\text{Al}_2\text{O}_3$  or (initially) amorphous alumina may be more appropriate. Amorphous  $\text{Al}_2\text{O}_3$  shows promising performance under ion irradiation [16], which probably persists as long as associated crystallisation and grain growth occur only in the nm range. It could also be argued that a polycrystalline material with preferential crystallographic orientation will generally suffer less from the effects of anisotropic swelling. In the spirit of what is mentioned above, any harmful effect of neutron irradiation on proper function of alumina as a TPB, without or after Li uptake, is irrelevant to application to the TER.

At the Karlsruhe Institute of Technology (KIT), the ECX process is being developed to provide steels, notably reduced-activation EUROFER, with a thin alumina layer on top of an aluminium-diffusion coating [17–20]. The eponymous, first process step is electroplating (electrochemical X deposition) aluminium onto the steel surface, followed by a heat treatment that is geared to the standard heat treatment of ferritic/martensitic EUROFER. The oxygen required for alumina formation stems from the heat-treatment atmosphere, which, for the ECX process, typically is flowing technical argon. The produced coatings show no signs of corrosion attack caused by flowing eutectic Li–Pb (550 °C, 0.1 m/s), still after exposure for 10,000 h [17], which strongly indicates that an alumina surface layer is present rather than oxides of iron or chromium (constituent elements of the substrate steel) have formed. However, this surface layer is thin, clearly  $< 1 \mu\text{m}$ , so that the capability of the coating with respect to reducing hydrogen permeation is quite limited. This has motivated the work described in the following, targeting at raising thicker alumina during the heat treatment of electroplated EUROFER. Examples of thermally grown alumina with thickness of a few  $\mu\text{m}$  have been reported, e.g., for heat treatments in air at 1000 °C [21] or 20–30 ppm (by volume) oxygen in argon at 700 °C ( $\gamma$ - $\text{Al}_2\text{O}_3$  [22]).

## 2. Experimental

The substrate on which ECX coatings with variation of the heat treatment are produced is ferritic/martensitic steel EUROFER 97 [23] with nominally 9 % (by mass) chromium, in the form of either  $\text{O}35 \times 1$  mm discs or  $\text{O}8 \times 24$  mm cylinders for later tests on performance with respect to hydrogen-isotope permeation and compatibility with liquid eutectic Li–Pb, respectively. In their original configuration, the discs have a flat extension for holding this samples during electroplating and heat treatment, which is afterwards cut off, and a piece of which ( $\sim 5 \times 3 \times 1$  mm) prepared for examination in the scanning electron microscope (SEM). On each one coated disc with different heat treatment (see below), X-ray diffraction spectroscopy (XRD) is performed, whereas an additionally electroplated piece of thin EUROFER sheet is examined with grazing-incidence XRD ( $3^\circ$ ) before and after each of the three stages of the standard heat treatment in argon.

Electroplating of aluminium as performed as the first step in the ECX process is illustrated in Fig. 1. In contrast to earlier reports [17–20], the operating temperature and average current density are chosen 110 °C and 15 mA per  $\text{cm}^2$  of substrate surface, respectively, and mechanical activation of the substrate surface abandoned in favour of chemical activation with inorganic acids (50 °C, 5–10 min). Each sample is plated for about 15 min in pulsed-current mode, corresponding to a theoretical thickness of deposited aluminium of 5  $\mu\text{m}$ . During aluminium deposition, the discs are masked on one side and not being moved in the static liquid electrolyte, whereas the cylinders rotate at low speed. The voltage between reference electrode and sample decreases from about  $-0.1$  to  $-0.6$  V for zero and peak current density ( $30 \text{ mA/cm}^2$ ), respectively.

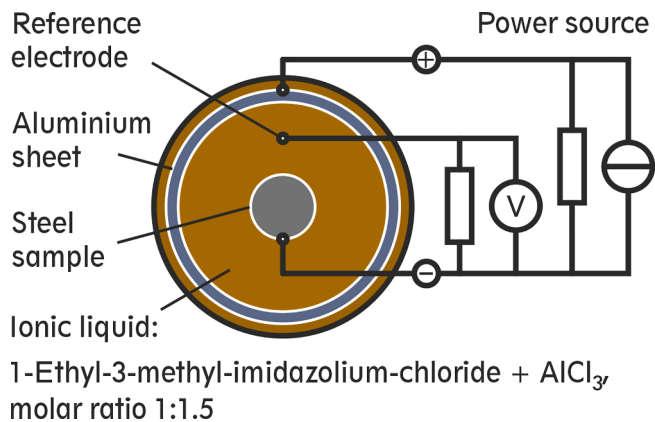


Fig. 1. Schematic illustration of electroplating of aluminium as performed as the first step in the ECX process.

The different three-stage heat treatments tried to increase the thickness of the alumina top layer on the ECX coating are listed in Table 1, along with the parameters of the standard treatment. The first stage at 640 °C (4 h, Ar flow) serves for interdiffusion of aluminium and steel elements below the aluminium melting point [24], and remains unaltered. Same for the temperature during the subsequent stages, i.e., 980 °C and 760 °C, respectively, which correspond to the standard heat treatment of EUROFER, in order to maintain or restore appropriate thermo-mechanical properties in the steel volume. Modifications are currently confined to the heat-treatment atmosphere (air instead of argon) during the second and third stage and holding time at 980 °C. The latter shall provide more time for nucleation and growth of alumina, which is likely to occur primarily after the formation of faster growing oxides of the constituent parts of the steel elements such as iron and chromium [25], which may reach the coating surface during the first stage of the heat treatments. The higher oxygen content in air in comparison to technical argon generally promotes the growth of oxides, however, unselectively with regard to the type of oxide.

## 3. Results and discussion

Fig. 2 shows cross sections of the produced aluminium-diffusion coatings as appearing in the SEM at medium magnification. For the standard heat treatment in argon, an oxide layer on top of the coating is hardly visible (Fig. 2a), whereas changing the atmosphere during the second (980 °C) and third stage (760 °C) from flowing argon to static air results in 1–2  $\mu\text{m}$  of surface oxide (Fig. 2b–d). Energy-dispersive X-ray spectroscopy (EDS), which comply qualitatively with element concentration profiles published earlier [20], discloses clearly aluminium-rich oxide for the three different times of holding at 980 °C in air, besides about 40 and 70  $\mu\text{m}$  aluminium penetration into the substrate steel, counted from the coating surface, for 0.5 and 2 h holding at 980 °C, respectively. Especially for 2 h at 980 °C, the oxide locally protrudes into

Table 1

Parameters of three-stage heat treatments of aluminium deposited on EUROFER substrate at 640, 980 and 760 °C, respectively: Time, atmosphere, cooling (C1: in cold furnace section, Ar stream; C2: air cooling outside furnace).

	Temperature (°C)		
	640	980	760
Standard	4 h, Ar, C1	0.5 h, Ar, C1	1.5 h, Ar, C1
Mod. 1	4 h, Ar, C1	0.5 h, air, C2	1.5 h, air, C2
Mod. 2	4 h, Ar, C1	1 h, air, C2	1.5 h, air, C2
Mod. 3	4 h, Ar, C1	2 h, air, C2	1.5 h, air, C2

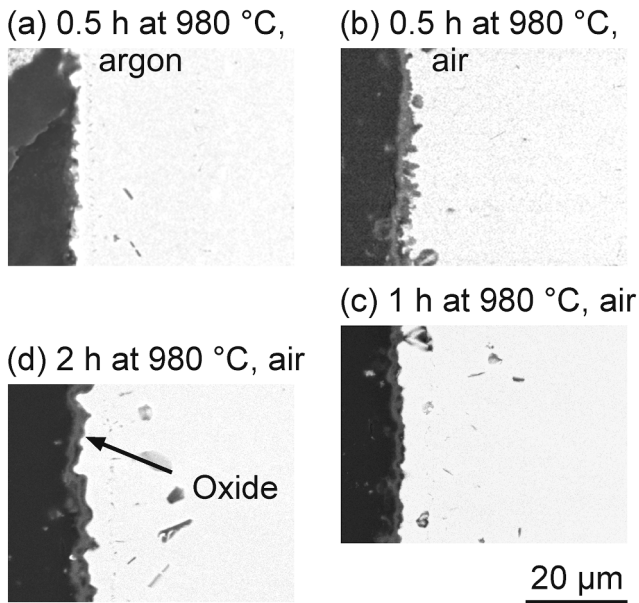


Fig. 2. Surface oxide as revealed by SEM on cross sections of ECX-coated EUROFER with (a) standard heat treatment in argon and (b–d) modified heat treatment.

the underlying material and interlocks the surface layer with the metallic portion of the coating (Fig. 2d), which is considered beneficial to oxide adherence [26].

Grazing-incidence XRD performed before and after each of the three stages of the standard heat treatment in argon identifies the evolution of the phases present in the near-surface part of the ECX coating. After electroplating (Fig. 3a), this clearly is aluminium, changing into intermetallic  $\text{Fe}_2\text{Al}_5$  by interdiffusion of aluminium and the elements in the substrate steel during the first stage of the heat treatment (Fig. 3b). At 980 °C (0.5 h),  $\text{Fe}_2\text{Al}_5$  dissolves to the benefit of an iron–aluminium solid solution (Fig. 3c), or an ordered solid solution such as  $\text{Fe}_3\text{Al}$ , which may

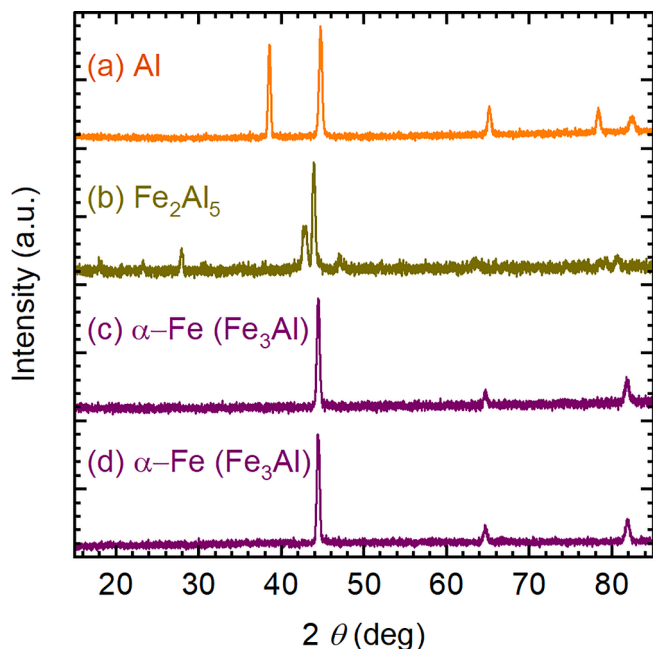


Fig. 3. Primary phases identified with the aid of grazing-incidence ( $3^\circ$ ) XRD on ECX coated EUROFER after (a) electroplating; (b) 4 h at 640 °C, argon; (c) 0.5 h at 980 °C, argon; and (d) another 1.5 h at 760 °C in argon.

be neither confirmed nor excluded by the XRD analysis alone. During the tempering stage (760 °C, 1.5 h), there seems to be no major phase transition in the near-surface portion of the coating anymore (Fig. 3d). Fig. 3d also corroborates that any surface oxide formed during the standard heat treatment in argon is too thin to be assessed by XRD. This clearly changes with performing the second and third stage in air (Fig. 4). The primarily formed oxide is likely to be  $\alpha\text{-Al}_2\text{O}_3$ , along with some iron or chromium oxide. In XRD spectra recorded after the modified heat treatments, the intensity of peaks associated to  $\alpha\text{-Al}_2\text{O}_3$  gradually increases with increasing time of holding at 980 °C, indicating increasing amount or thickness of this oxide. For evaluation of the recorded XRD spectra, inter alia, the following reference patterns were consulted: aluminium [27],  $\text{Fe}_2\text{Al}_5$  [28], ferrite ( $\alpha\text{-Fe}$ ) [29],  $\text{Fe}_3\text{Al}$  [30],  $\alpha\text{-Al}_2\text{O}_3$  [31],  $\alpha\text{-Fe}_2\text{O}_3$  [32],  $\alpha\text{-Cr}_2\text{O}_3$  [33].

As an alumina layer should not be affected by liquid eutectic Li–Pb beyond some uptake of lithium (whereby integrity of the layer is not lost in the sense that corrosion of underlying material occurs [21,34]), exposure to the liquid metal primarily is a benchmark for the quality in terms of continuity and absence of remarkable defects. Such exposure of the four ECX coatings with different heat treatment (Table 1) for 3000 h to Li–Pb at 550 °C in the PICOLO loop, however, under low-flow to stagnant conditions, largely reveals a protective coating as exemplified in Fig. 5a. Weak spots occur at frequencies that, according to qualitative evaluation of each one cross section in the light-optical and scanning electron microscope, are lower after heat treatments performed in air, in comparison to the standard treatment in argon, and decrease with increasing time of holding at 980 °C in air. Especially for the heat treatments partly performed in air, imperfect performance of the oxide layer has led to accumulation of the liquid metal underneath the oxide, and associated degradation is confined to the coating rather than reaching the substrate steel. Where the surface oxide failed and corrosion of the underlying metal occurred, remnants of convoluted alumina are conserved in solidified Li–Pb, which correspond to the wrinkled oxide found in locations exemplified in Fig. 5b. The latter exhibit a relatively non-uniform and ragged surface of the metallic portion of the coating, suggesting local melt formation during the heat treatment. Partial melting of the deposited aluminium may come about during the second stage of the heat treatments at 980 °C, if transformation into aluminides during the first stage at 640 °C, below the melting point of aluminium, was incomplete.

Besides the surface layer, Fig. 5a highlights the two portions of the metallic part of the (diffusion) coating: The one next to the oxide layer is characterised by approximately constant aluminium concentration (possibly  $\text{Fe}_3\text{Al}$ ; Fig. 3), followed by an aluminium-diffusion zone. The

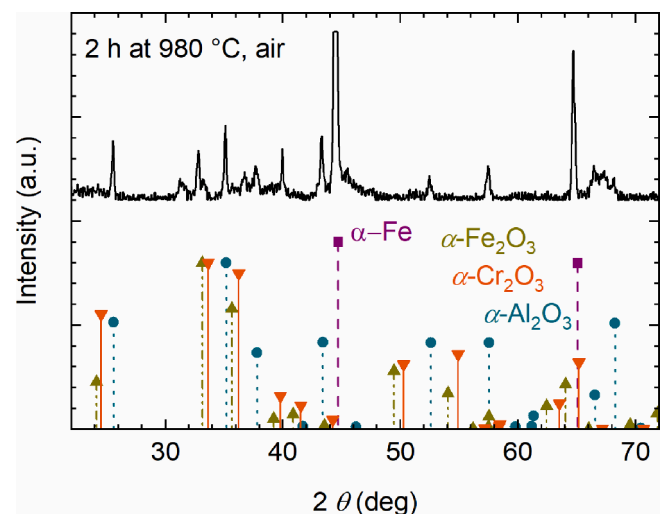
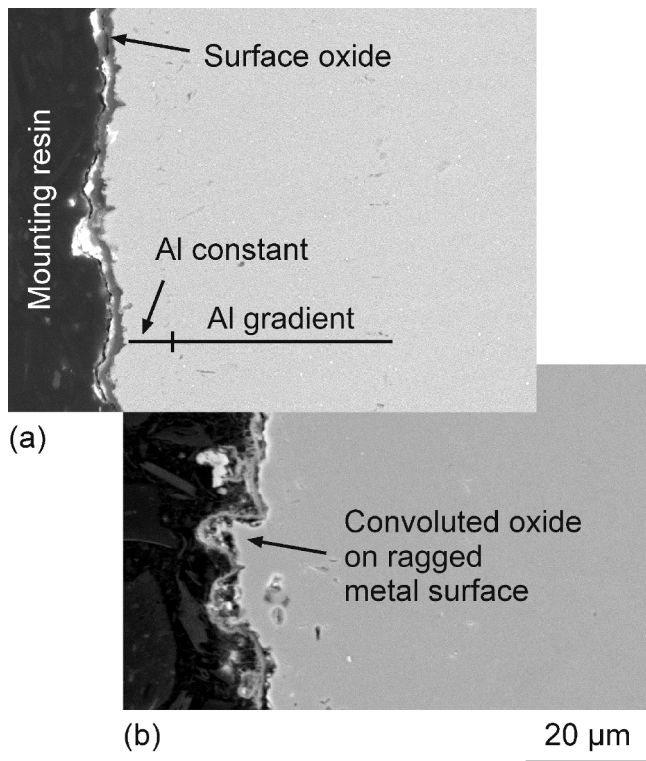


Fig. 4. XRD spectrum and attribution of observed peaks for ECX coating with modified heat treatment, namely 2 h at 980 °C in air.



**Fig. 5.** Electron-optical micrograph of ECX coating with heat treatment Mod. 2 (Table 1) after exposure for 3000 h to eutectic Li–Pb: (a) Oxide layer apparently persistent where the surface of the metallic portion of the coating is relatively smooth, and (b) wrinkled and convoluted oxide on rather non-uniform, ragged metal surface.

penetration depth of aluminium after 3000 h at 550 °C is around 50 µm, irrespective of the heat treatment during production of the coating. Some inconsistencies with penetration depth as observed on the flat substrate (1 mm) immediately after the heat treatments (see above) may tentatively be explained with the thicker substrate (Ø8 mm) used to produce the samples for exposure to Li–Pb. Just as for coatings before exposure to Li–Pb, EDS element concentration profiles correspond to what has been published earlier [17,19]. Bright spots in the substrate and metallic part of the coating (Fig. 5) hint at precipitates enriched in heavy metals such as tantalum or tungsten, appearing to be somewhat larger here than described for as-delivered EUROFER steel [35].

#### 4. Conclusions

Though changing the heat-treatment atmosphere from argon to air has the anticipated effect with respect to the amount of alumina formed, the preliminary results from exposure to Li–Pb indicate some local defects being present in the oxide for all heat treatments tested. At this stage, these defects are suspected in the convoluted oxide layers that form where the surface of the metallic portion of the diffusion coatings is rather non-uniform and ragged. Attributing the latter to partial melt formation during the heat treatments, suggests prolonging the first stage at 640 °C as a remedy. As for raising thicker alumina by performing the subsequent stages of the heat treatment in air instead of argon, 0.5 h at 980 °C, which corresponds to the standard treatment of EUROFER, suffices to produce 1–2 µm of the oxide, which is already in the same range as after 2 h at this temperature in air. Meeting concerns that the  $\alpha$ -Al<sub>2</sub>O<sub>3</sub> formed by heat treatments so far investigated for ECX coatings, finally, seems to be applicable as a tritium-permeation barrier only to the TER of the breeding blanket, heat treatments could be geared to raising  $\gamma$ -Al<sub>2</sub>O<sub>3</sub> [22], with presumably better performance under neutron irradiation.

#### CRediT authorship contribution statement

**Carsten Schroer:** Conceptualization, Formal analysis, Methodology, Supervision, Writing – original draft, Writing – review & editing. **Julia Lorenz:** Investigation. **Olaf Wedemeyer:** Investigation. **Aleksandr Skrypnik:** Investigation. **Kateryna Khanchych:** Investigation.

#### Declaration of competing interest

The authors declare the following financial interests/personal relationships which may be considered as potential competing interests: Kateryna Khanchych reports financial support was provided by Helmholtz Initiative for Refugees (Funding Code GI-027). Carsten Schroer reports financial support was provided by EUROfusion (Grant Agreement No 101052200). If there are other authors, they declare that they have no known competing financial interests or personal relationships that could have appeared to influence the work reported in this paper.

#### Data availability

Data will be made available on request.

#### Acknowledgements

The authors would like to thank Drs. A. Heinzel (KIT-IHM) and K. Seemann (KIT-IAM-AWP) for conducting and evaluating XRD measurements. Financial support by the Nuclear Fusion Programme (FUSION) of KIT as well as the Helmholtz Initiative for Refugees is gratefully acknowledged.

This work has been carried out within the framework of the EUROfusion Consortium, funded by the European Union via the Euratom Research and Training Programme (Grant Agreement No 101052200 – EUROfusion). Views and opinions expressed are however those of the author(s) only and do not necessarily reflect those of the European Union or the European Commission. Neither the European Union nor the European Commission can be held responsible for them.

We acknowledge support by the KIT-Publication Fund of the Karlsruhe Institute of Technology.

#### References

- [1] J. Ongena, R. Koch, R. Wolf, H. Zohm, *Nature Phys.* 12 (2016) 398–410, <https://doi.org/10.1038/NPHYS3745>.
- [2] E.C.E. Rönnebro, R.L. Oelrich, R.O. Gates, *Molecules* 27 (2022), <https://doi.org/10.3390/molecules27196528>.
- [3] V. Nemanic, *Nucl. Mater. Energy* 19 (2019) 451–457, <https://doi.org/10.1016/j.nme.2019.04.001>.
- [4] T. Chikada, *Ceramic coatings for fusion reactors*, in: R. Konings, R.E. Stoller (Eds.), *Comprehensive Nuclear Materials*, 2nd ed., Elsevier, 2020, pp. 274–283.
- [5] C.H. Henager Jr., *Hydrogen permeation barrier coatings*, in: R.H. Jones, G.J. Thomas (Eds.), *Materials for the Hydrogen Economy*, CRC Press, Boca Raton, FL, 2007, Chapter 8 (10 pages).
- [6] R.A. Causey, R.A. Karnesky, C. San Marchi, *Tritium barriers and tritium diffusion in fusion reactors*, in: R.J.M. Konings, T.R. Allen, R.E. Stoller, S. Yamanaka (Eds.), *Comprehensive Nuclear Materials* 4, Elsevier, Amsterdam, 2012, pp. 511–549.
- [7] F. Cismondi, G.A. Spagnuolo, L.V. Boccaccini, P. Chiovaro, S. Ciattaglia, I. Cristescu, C. Day, A. Del Nevo, P.A. Di Maio, G. Federici, F. Hernandez, C. Moreno, I. Moscato, P. Pereslavtsev, D. Rapisarda, A. Santucci, M. Utili, *Fusion Eng. Des.* 157 (2020) 111640, <https://doi.org/10.1016/j.fusengdes.2020.111640>.
- [8] J. Jun, K.A. Unocic, M.J. Lance, H.M. Meyer, B.A. Pint, *J. Nucl. Mater.* 528 (2020) 151847, <https://doi.org/10.1016/j.jnucmat.2019.151847>.
- [9] B.A. Pint, J.L. Moser, A. Jankowski, J. Hayes, *J. Nucl. Mater.* 367–370 (2007) 1165–1169, <https://doi.org/10.1016/j.jnucmat.2007.03.208>.
- [10] A. Houben, M. Rasiński, L. Gao, C. Linsmeier, *Nucl. Mater. Energy* 24 (2020) 100752, <https://doi.org/10.1016/j.nme.2020.100752>.
- [11] M. Utili, S. Bassini, S. Cataldo, F. Di Fonzo, M. Kordac, T. Hernandez, K. Kunzova, J. Lorenz, D. Martelli, B. Padino, A. Moroño, M. Tarantino, C. Schroer, G. A. Spagnuolo, L. Vala, M. Vanazzi, A. Venturini, *Fusion Eng. Des.* 170 (2021) 112453, <https://doi.org/10.1016/j.fusengdes.2021.112453>.
- [12] I. Levin, D. Brandon, *J. Am. Ceram. Soc.* 81 (1998) 1995–2012, <https://doi.org/10.1111/j.1151-2916.1998.tb02581.x>.
- [13] K. Wefers, C. Misra, *Oxides and Hydroxides of Aluminum*, Alcoa Technical Paper 19, revised, Aluminum Company of America, Pittsburgh, PA, 1987.

- [14] A. Bhattacharya, S.J. Zinkle, Cavity swelling in irradiated materials, in: R. Konings, R.E. Stoller (Eds.), *Comprehensive Nuclear Materials*, 2nd ed., Elsevier, 2020, pp. 406–455.
- [15] P. Hubberstey, *J. Nucl. Mater.* 247 (1997) 208–214, [https://doi.org/10.1016/S0022-3115\(97\)00071-8](https://doi.org/10.1016/S0022-3115(97)00071-8).
- [16] F. García Ferré, A. Mairov, M. Vanazzi, Y. Serruys, F. Leprêtre, L. Beck, L. van Brutzel, A. Chartier, M.G. Beghi, K. Sridharan, F. Di Fonzo, *Acta Mater.* 143 (2018) 156–165, <https://doi.org/10.1016/j.actamat.2017.10.011>.
- [17] S.-E. Wulf, W. Krauss, J. Konys, *Nucl. Mater. Energy* 16 (2018) 158–162, <https://doi.org/10.1016/j.nme.2018.06.019>.
- [18] S.-E. Wulf, W. Krauss, J. Konys, *Fusion Eng. Des.* 124 (2017) 1091–1095, <https://doi.org/10.1016/j.fusengdes.2017.03.115>.
- [19] S.-E. Wulf, W. Krauss, J. Konys, *Nucl. Mater. Energy* 9 (2016) 519–523, <https://doi.org/10.1016/j.nme.2016.03.008>.
- [20] S.-E. Wulf, N. Holstein, W. Krauss, J. Konys, *Fusion Eng. Des.* 88 (2013) 2530–2534, <https://doi.org/10.1016/j.fusengdes.2013.05.060>.
- [21] B.A. Pint, K.L. More, *J. Nucl. Mater.* 376 (2008) 108–113, <https://doi.org/10.1016/j.jnucmat.2007.12.010>.
- [22] G. Zhang, F. Yang, G. Lu, X. Xiang, T. Tang, X. Wang, *J. Fusion Energ.* 37 (2018) 317–324, <https://doi.org/10.1007/s10894-018-0201-2>.
- [23] R. Lindau, A. Möslang, M. Rieth, M. Klimiankou, E. Materna-Morris, A. Alamo, A.-A.-F. Tavassoli, C. Cayron, A.-M. Lancha, P. Fernandez, N. Baluc, R. Schäublin, E. Diegele, G. Filacchioni, J.W. Rensman, B. Schaaf, E. Lucon, W. Dietz, *Fusion Eng. Des.* 75–79 (2005) 989–996, <https://doi.org/10.1016/j.fusengdes.2005.06.186>.
- [24] K. Bhanumurthy, W. Krauss, J. Konys, *Fusion Sci. Technol.* 65 (2014) 262–272, <https://doi.org/10.13182/FST13-651>.
- [25] F.H. Stott, *Mater. Sci. Technol.* 5 (1989) 734–740, <https://doi.org/10.1179/mst.1989.5.8.734>.
- [26] G.C. Wood, F.H. Stott, *Mater. Sci. Technol.* 3 (1987) 519–530, <https://doi.org/10.1080/02670836.1987.11782263>.
- [27] M.E. Straumanis, *J. Appl. Phys.* 30 (1959) 1965–1969, <https://doi.org/10.1063/1.1735098>.
- [28] U. Burkhardt, Y. Grin, M. Ellner, K. Peters, *Acta Crystallogr. B Struct. Sci.* 50 (1994) 313–316, <https://doi.org/10.1107/S0108768193013989>.
- [29] M.E. Straumanis, D.C. Kim, *Int. J. Mater. Res.* 60 (1969) 272–277, <https://doi.org/10.1515/ijmr-1969-600404>.
- [30] A.J. Bradley, A.H. Jay, *J. Iron Steel Instit., London* 125 (1932) 339–357.
- [31] H. Sawada, *Mater. Res. Bul.* 29 (1994) 127–133, [https://doi.org/10.1016/0025-5408\(94\)90132-5](https://doi.org/10.1016/0025-5408(94)90132-5).
- [32] A.H. Hill, F. Jiao, P.G. Bruce, A. Harrison, W. Kockelmann, C. Ritter, *Chem. Mater.* 20 (2008) 4891–4899, <https://doi.org/10.1021/cm800009s>.
- [33] H. Sawada, *Mater. Res. Bul.* 29 (1994) 239–245, [https://doi.org/10.1016/0025-5408\(94\)90019-1](https://doi.org/10.1016/0025-5408(94)90019-1).
- [34] B.A. Pint, L.R. Walker, K.A. Unocic, *Mater. High Temp.* 29 (2012) 129–135, <https://doi.org/10.3184/096034012X1333452977329>.
- [35] M. Klimenkov, R. Lindau, E. Materna-Morris, A. Möslang, *Prog. Nucl. Energy* 57 (2012) 8–13, <https://doi.org/10.1016/j.pnucene.2011.10.006>.